Inverse kinematics for optimal tool orientation control in 5-axis CNC machining

Rida T. Farouki,[1] Chang Yong Han,[2] and Shiqiao Li[1]

[1] Department of Mechanical and Aerospace Engineering, University of California, Davis, CA 95616, USA

[2] Department of Applied Mathematics, Kyung Hee University, Yongin–si, Gyeonggi–do 446–701, SOUTH KOREA

Abstract

The problem of determining the inputs to the rotary axes of a 5–axis CNC machine is addressed, such that relative variations of orientation between the tool axis and surface normal are minimized subject to the constraint of maintaining a constant cutting speed with a ball-end tool. In the context of an orientable–spindle machine, the results of a prior study are directly applicable to the solution of this inverse–kinematics problem. However, since they are expressed in terms of the integral of the geodesic curvature, a discrete time–step solution is proposed that yields accurate rotary–axis increments at high sampling frequencies. For an orientable–table machine, a closed–form solution that specifies the rotary–axis positions as functions of the surface normal variation along the toolpath is possible. In this context, however, the feasibility of a solution is dependent upon the surface normal along the toolpath satisfying certain orientational constraints. These inverse–kinematics solutions facilitate accurate and efficient 5–axis machining of free–form surfaces without "unnecessary" actuation of the machine rotary axes.

keywords: 5–axis CNC machining; tool orientation; inverse kinematics; ball–end tool; orientable–spindle machine; orientable–table machine.

e–mail: farouki@ucdavis.edu, cyhan@khu.ac.kr, shqli@ucdavis.edu

1 Introduction

A 5–axis CNC machine incorporates three translational and two rotational degrees of freedom to maintain the desired relative position and orientation of the cutting tool and workpiece during the execution of a part program. The rotary axes of 5–axis machines permit more intricate part shapes to be cut, without re–fixturing of the workpiece, than with 3–axis machines. However, the development of part programs for accurate and efficient 5–axis machining of free–form surfaces is a challenging problem [2, 8, 10, 11, 12, 17, 18, 22, 23] for which fully–automated solutions have remained elusive — see Section 2 of [6] for a more comprehensive review of the literature.

The problem of orienting the tool axis $\mathbf{a}$ with respect to the surface normal $\mathbf{n}$ along a smooth curve on the surface, so as to minimize orientational changes while satisfying (for a given angle ψ) the fixed cutting speed condition $\mathbf{a} \cdot \mathbf{n} = \cos\psi$, was considered in [6]. It was observed that, in the workpiece (x, y, z) coordinate system, the solution to this problem corresponds to specifying the orientation of the tangent–plane component $\mathbf{a}_t = \mathbf{a} - \cos\psi\, \mathbf{n}$ of $\mathbf{a}$ relative to the Darboux frame by an angle ϕ specified (modulo a constant) by minus the integral of the geodesic curvature with respect to arc length along the curve. Equivalently, $\mathbf{a}_t$ has no instantaneous rotation about the surface normal.

The optimal tool orientation strategy proposed in [6] is directly applicable to an *orientable–spindle machine*, in which the workpiece maintains a fixed orientation, and the rotary axes control the tool orientation. In an *orientable–table machine*, on the other hand, the tool maintains a fixed orientation, and the rotary axes control the orientation of the table upon which the workpiece is mounted. For both types of machine, the *inverse kinematics* problem for the rotational axes must be solved, i.e., within each sampling interval of the digital controller, the angular positions of those axes must be determined so as to maintain the desired relative tool/workpiece orientation.

In general, finite spatial rotations about distinct axes do not commute — i.e., the end result depends on the *order* in which the rotations are performed. However, for the specific configurations of orientable–spindle and orientable–table machines — with one stationary rotation axis, and the second rotation axis mounted upon (and moving with) it — finite axis rotations do commute, so their order is unimportant. The transformation of a vector specified with the machine axes in "home" position to a general machine orientation can thus be described by a single rotation matrix that depends on two angular parameters, namely, the rotary–axis inputs. This fact facilitates a solution of

the inverse–kinematics problem, for both orientable–spindle and orientable–table machines, so as to achieve the desired relative orientation of $\mathbf{a}$ and $\mathbf{n}$ at each point along a prescribed toolpath on a smooth surface.

The remainder of this paper is organized as follows. The basic problem of optimal tool/workpiece orientation control, under the constraint of a constant cutting speed using a ball–end tool, is introduced in Section 2 in the context of both orientable–spindle and orientable–table machines. Some background differential geometry of paths on smooth surfaces is then briefly reviewed in Section 3. In Section 4, the canonical configurations of the rotational axes on orientable–spindle and orientable–table machines are described, and a matrix formulation for general spatial rotations is presented. Section 5 addresses the inverse–kinematics solution for orientable–spindle machines, using the results from [6]. Since the solution involves the integral of the geodesic curvature with respect to arc length along the toolpath, which does not generally admit a closed–form reduction, a discrete time–step method is proposed that yields accurate results for sufficiently high sampling rates. The inverse kinematics of orientable–table machines, considered in Section 6, is simpler and admits a general closed–form solution for the rotary–axis inputs, expressed only in terms of the surface normal variation along the toolpath. Finally, Section 7 summarizes the main results of the present study, and identifies some open problems that warrant further investigation.

2 Optimal tool/workpiece orientation

The problem addressed herein concerns the specification of tool orientation in 5–axis machining of free–form shapes with a spherical or "ball–end" tool of given radius R. Such a tool permits gouge–free machining of any surface with smallest concave principal radius of curvature not less than R. If the tool has angular speed n rpm and $0 < \psi < \frac{1}{2}\pi$ is the angle between the tool axis $\mathbf{a}$ and the surface normal $\mathbf{n}$ at the contact point, the cutting speed is

$$v_c \;=\; \frac{2\pi n}{60}\, R \sin\psi \,.$$

Thus, to maintain a constant cutting speed, the polar angle of $\mathbf{a}$ with respect to $\mathbf{n}$ (or $\mathbf{n}$ with respect to $\mathbf{a}$) must be equal to ψ, but the azimuthal angle of $\mathbf{a}$ with respect to $\mathbf{n}$ (or $\mathbf{n}$ with respect to $\mathbf{a}$) remains indeterminate.

The methodology proposed in [6] achieves "optimal" satisfaction of the constant cutting–speed condition, by eliminating any relative motion between

a and **n** that is superfluous to its maintenance. Choosing the surface normal **n** as a reference, as in [6], means that the component of **a** parallel to **n** is $\mathbf{a}_\parallel = \cos\psi\,\mathbf{n}$, while the perpendicular component $\mathbf{a}_\perp = \mathbf{a} - \mathbf{a}_\parallel$ should exhibit no instaneous rotation about **n**. This interpretation is directly applicable to the orientable–spindle machine context. In the context of an orientable–table machine, however, it is more convenient to choose the (stationary) tool axis **a** as a reference: we then require the component of the surface normal **n** parallel to **a** to be $\mathbf{n}_\parallel = \cos\psi\,\mathbf{a}$, while the perpendicular component $\mathbf{n}_\perp = \mathbf{n} - \mathbf{n}_\parallel$ should exhibit no instaneous rotation about **a**.

For the orientable–spindle machine, it was shown in [6] that the desired motion is realized if **a** is specified as a fixed vector in an orthonormal frame $(\mathbf{n}, \mathbf{v}, \mathbf{w})$ that is *rotation–minimizing*[1] with respect to **n** — i.e., its angular velocity $\boldsymbol{\omega}$ must satisfy $\boldsymbol{\omega} \cdot \mathbf{n} \equiv 0$. The tangent–plane vectors of such a frame have an angular orientation ϕ, relative to the tangent–plane vectors of the Darboux frame, specified (modulo a constant) by minus the integral of the geodesic curvature with respect to the toolpath arc length — see Section 3. As described in Section 5, this result facilitates determination of the rotary–axis inputs for the orientable–spindle machine in terms of ϕ. However, since the integral defining ϕ does not in general admit analytic reduction, a discrete time–step scheme for the rotary–axis inputs is also developed in Section 5, appropriate to controllers with sufficiently high sampling frequencies.

For the orientable–table machine, the inverse–kinematics formulation is in some respects simpler than for the orientable–spindle machine, since the tool axis vector is stationary and only the workpiece orientation is varied to achieve the desired relative behavior of **a** and **n**. In fact, when $\mathbf{n}_\parallel = \cos\psi\,\mathbf{a}$ and $\mathbf{n}_\perp = \mathbf{n} - \mathbf{n}_\parallel$ has no instantaneous rotation about **a** for a fixed vector **a**, it is clear that the workpiece orientation must vary such as to make the surface normal **n** at each point of the toolpath coincide with some fixed vector $\mathbf{n}_0$. The integral ϕ is not required in this context, and a closed–form solution for the rotary–axis inputs is possible, as described in Section 6.

3 Geometry of surface toolpaths

Consider a curve $\mathbf{r}(\xi) = \mathbf{s}(u(\xi), v(\xi))$ on a smooth surface $\mathbf{s}(u, v)$ defined by expressing the surface parameters u, v as functions of a path parameter ξ.

[1] Rotation–minimizing frames have been studied [1, 3, 4, 5, 9, 14, 21] in the context of applications to computer animation, spatial motion design, and swept surface construction.

Differentiating by the chain rule gives

$$\mathbf{r}'(\xi) \,=\, u'(\xi)\,\mathbf{s}_u(u(\xi),v(\xi)) \,+\, v'(\xi)\,\mathbf{s}_v(u(\xi),v(\xi))$$

where $\mathbf{s}_u$, $\mathbf{s}_v$ are the partial derivatives of $\mathbf{s}(u,v)$. The parametric speed of $\mathbf{r}(\xi)$ — i.e., the rate of change of arc length s with the parameter ξ — is

$$\sigma \,=\, \frac{\mathrm{d}s}{\mathrm{d}\xi} \,=\, |\,\mathbf{r}'\,| \,=\, |\,u'\,\mathbf{s}_u + v'\,\mathbf{s}_v\,|\,. \tag{1}$$

Assuming that $\mathbf{s}_u \times \mathbf{s}_v \neq \mathbf{0}$ everywhere, the unit surface normal is defined at each point by

$$\mathbf{n} \,=\, \frac{\mathbf{s}_u \times \mathbf{s}_v}{|\,\mathbf{s}_u \times \mathbf{s}_v\,|}\,. \tag{2}$$

The *Darboux frame* $(\mathbf{n},\mathbf{t},\mathbf{u})$ along the curve $\mathbf{r}(\xi) = \mathbf{s}(u(\xi),v(\xi))$ is a set of three orthonormal vectors, where the surface normal $\mathbf{n}$ is defined by (2), the *tangent* to the curve $\mathbf{r}(\xi)$ is specified as

$$\mathbf{t} \,=\, \frac{\mathbf{r}'}{|\,\mathbf{r}'\,|} \,=\, \frac{u'\,\mathbf{s}_u + v'\,\mathbf{s}_v}{|\,u'\,\mathbf{s}_u + v'\,\mathbf{s}_v\,|}\,, \tag{3}$$

and the *tangent normal* $\mathbf{u}$ is a vector in the surface tangent plane orthogonal to $\mathbf{t}$, defined by

$$\mathbf{u} \,=\, \mathbf{n} \times \mathbf{t}\,. \tag{4}$$

The variation of the Darboux frame is described by the equations

$$\begin{bmatrix} \mathbf{n}' \\ \mathbf{t}' \\ \mathbf{u}' \end{bmatrix} \,=\, \sigma \begin{bmatrix} 0 & -\kappa_{\mathrm{n}} & \tau_{\mathrm{g}} \\ \kappa_{\mathrm{n}} & 0 & \kappa_{\mathrm{g}} \\ -\tau_{\mathrm{g}} & -\kappa_{\mathrm{g}} & 0 \end{bmatrix} \begin{bmatrix} \mathbf{n} \\ \mathbf{t} \\ \mathbf{u} \end{bmatrix}\,, \tag{5}$$

where the quantities

$$\kappa_{\mathrm{n}} \,=\, \frac{\mathbf{n}\cdot\mathbf{t}'}{\sigma}\,, \qquad \kappa_{\mathrm{g}} \,=\, \frac{\mathbf{u}\cdot\mathbf{t}'}{\sigma}\,, \qquad \tau_{\mathrm{g}} \,=\, \frac{\mathbf{u}\cdot\mathbf{n}'}{\sigma} \tag{6}$$

define the *normal curvature*, *geodesic curvature*, and *geodesic torsion* [15, 20] along the path $\mathbf{r}(\xi) = \mathbf{s}(u(\xi),v(\xi))$. The relations (5) can be expressed as

$$\mathbf{n}' \,=\, \sigma\,\boldsymbol{\Omega} \times \mathbf{n}\,, \qquad \mathbf{t}' \,=\, \sigma\,\boldsymbol{\Omega} \times \mathbf{t}\,, \qquad \mathbf{u}' \,=\, \sigma\,\boldsymbol{\Omega} \times \mathbf{u}\,,$$

where the *angular velocity* $\mathbf{\Omega}$ of the Darboux frame [15, 20] along $\mathbf{r}(\xi)$ is

$$\mathbf{\Omega} \,=\, \kappa_{\rm g}\,\mathbf{n} \,-\, \tau_{\rm g}\,\mathbf{t} \,-\, \kappa_{\rm n}\,\mathbf{u}\,. \tag{7}$$

In lieu of $\mathbf{t}$ and $\mathbf{u}$, we introduce new basis vectors $\mathbf{v}$ and $\mathbf{w}$ for the surface tangent plane, defined by

$$\mathbf{v} \,=\, \cos\phi\,\mathbf{t} + \sin\phi\,\mathbf{u}\,, \qquad \mathbf{w} \,=\, -\,\sin\phi\,\mathbf{t} + \cos\phi\,\mathbf{u}\,, \tag{8}$$

with

$$\phi \,=\, \phi_0 - \int_0^\xi \kappa_{\rm g}\,\sigma\,{\rm d}\xi\,, \tag{9}$$

where ϕ_0 is an integration constant. With this choice, the derivatives

$$\mathbf{v}' \,=\, \sigma\,(\kappa_{\rm n}\cos\phi - \tau_{\rm g}\sin\phi)\,\mathbf{n}\,, \qquad \mathbf{w}' \,=\, -\,\sigma\,(\kappa_{\rm n}\sin\phi + \tau_{\rm g}\cos\phi)\,\mathbf{n} \tag{10}$$

of the tangent–plane vectors $\mathbf{v}$, $\mathbf{w}$ are always parallel to the surface normal $\mathbf{n}$. Equivalently, the orthonormal frame $(\mathbf{n}, \mathbf{v}, \mathbf{w})$ is *rotation–minimizing* with respect to $\mathbf{n}$ — i.e., if the variation of this frame is described by its angular velocity $\boldsymbol{\omega}$ such that

$$\mathbf{v}' \,=\, \sigma\,\boldsymbol{\omega}\times\mathbf{v}\,, \quad \mathbf{w}' \,=\, \sigma\,\boldsymbol{\omega}\times\mathbf{w}\,, \quad \mathbf{n}' \,=\, \sigma\,\boldsymbol{\omega}\times\mathbf{n}$$

then $\boldsymbol{\omega}\cdot\mathbf{n} \equiv 0$, so $\mathbf{v}$ and $\mathbf{w}$ exhibit no instantaneous rotation about $\mathbf{n}$.

Since $(\mathbf{v}, \mathbf{w}, \mathbf{n})$ is an orthonormal basis, $\mathbf{v}'$ and $\mathbf{w}'$ are parallel to $\mathbf{n}$ if and only if $\mathbf{v}\cdot\mathbf{v}' = \mathbf{w}\cdot\mathbf{v}' = 0$ and $\mathbf{v}\cdot\mathbf{w}' = \mathbf{w}\cdot\mathbf{w}' = 0$. Now $\mathbf{v}\cdot\mathbf{v}' = \mathbf{w}\cdot\mathbf{w}' = 0$ is a consequence of the fact that $\mathbf{v}$ and $\mathbf{w}$ are unit vectors. Also, differentiating $\mathbf{v}\cdot\mathbf{w} = 0$ gives $\mathbf{v}'\cdot\mathbf{w} + \mathbf{v}\cdot\mathbf{w}' = 0$, and hence $\mathbf{v}'\cdot\mathbf{w} = 0 \;\Leftrightarrow\; \mathbf{v}\cdot\mathbf{w}' = 0$. Thus, either of the conditions

$$\mathbf{v}'\cdot\mathbf{w} \,=\, 0 \qquad \text{or} \qquad \mathbf{v}\cdot\mathbf{w}' \,=\, 0 \tag{11}$$

suffices to ensure that the frame $(\mathbf{n}, \mathbf{v}, \mathbf{w})$ is rotation–minimizing with respect to $\mathbf{n}$. It is evident from (8) and (10) that these conditions are satisfied.

In [6] the tool axis vector $\mathbf{a}$ was specified in terms of the frame $(\mathbf{n}, \mathbf{v}, \mathbf{w})$ and a fixed angle ψ, determined by the desired cutting speed, as

$$\mathbf{a} \,=\, \cos\psi\,\mathbf{n} \,+\, \sin\psi\,\mathbf{v}\,. \tag{12}$$

Note that the angular velocity $\boldsymbol{\omega}$ of the frame $(\mathbf{n}, \mathbf{v}, \mathbf{w})$ — and thus of the tool axis vector $\mathbf{a}$ — is obtained by dropping the $\mathbf{n}$ component of the Darboux frame angular velocity (7), i.e., it is just

$$\boldsymbol{\omega} \,=\, -\,\tau_{\rm g}\,\mathbf{t} \,-\, \kappa_{\rm n}\,\mathbf{u}\,. \tag{13}$$

4 Inverse kinematics for rotary axes

During each sampling interval of the servosystem, the real–time interpolator for the rotary axes of a 5–axis CNC machine must determine the incremental axis rotations necessary to maintain a prescribed orientation of the cutting tool relative to the workpiece. Two canonical 5–axis machine configurations, the *orientable–spindle machine* and *orientable–table machine*, are considered here. The former employs a spindle of variable orientation and a workpiece table of fixed orientation, while the latter has a fixed–orientation spindle and a workpiece table whose orientation can be varied. These are two of three basic 5–axis machine configurations [13, 16, 19] — the third being a hybrid of the orientable–spindle and orientable–table forms, whose inverse kinematics can be deduced by suitable adaptation of the methods described below.

The configurations of the rotary axes of orientable–spindle and orientable–table machines are analogous to those of an altazimuth mount for a telescope or theodolite, with one fixed axis and a second axis that is mounted on the first and rotates with it, in the plane orthogonal to the first axis. Let (x, y, z) be a stationary coordinate system aligned with the machine translational axes and let $(\mathbf{i}, \mathbf{j}, \mathbf{k})$ be associated unit vectors. The orientable–spindle machine incorporates rotary a and b axes, aligned with the x and y directions when the machine is in "home" position. The angular positions of these axes, relative to home position, are denoted by α and β. The b rotary axis is attached to the machine frame and always aligned with the y direction, but the a rotary axis is mounted on the b axis and moves with it. The instantaneous sense of rotation associated with the a and b axes is thus defined by the unit vectors

$$\mathbf{m}_a \,=\, \cos\beta\,\mathbf{i} - \sin\beta\,\mathbf{k}\,, \qquad \mathbf{m}_b \,=\, \mathbf{j}\,. \tag{14}$$

The range of feasible positions for the rotary axes on the orientable–spindle machine are assumed to be $\alpha \in (-\frac{1}{2}\pi, +\frac{1}{2}\pi)$ and $\beta \in (-\frac{1}{2}\pi, +\frac{1}{2}\pi)$.

The orientable–table machine employs rotary c and a axes, aligned with the z and x directions in "home" position. The angular positions of these axes relative to home position are denoted by γ and α. The c axis is attached to the machine frame and always aligned with the z direction, but the a axis is mounted on the c axis and moves with it. Thus, the instantaneous sense of rotation associated with the c and a axis is defined by the unit vectors

$$\mathbf{m}_c \,=\, \mathbf{k}\,, \qquad \mathbf{m}_a \,=\, \cos\gamma\,\mathbf{i} + \sin\gamma\,\mathbf{j}\,. \tag{15}$$

The feasible positions of the rotary axes on the orientable–table machine are assumed to be $\gamma \in (-\pi, +\pi\,]$ and $\alpha \in (-\frac{1}{2}\pi, +\frac{1}{2}\pi)$.

The basic configurations of orientable–spindle and orientable–table 5–axis CNC machines are illustrated in Figure 1. In general, the result of two finite spatial rotations about distinct axes depends on the order in which they are applied. However, as shown in Sections 5 and 6 below, this problem does not arise with the specific rotary–axis configurations of an orientable–spindle or orientable–table machine — i.e., the current angular positions (α, β) or (γ, α) of the rotary axes uniquely determine the relative tool/workpiece orientation.

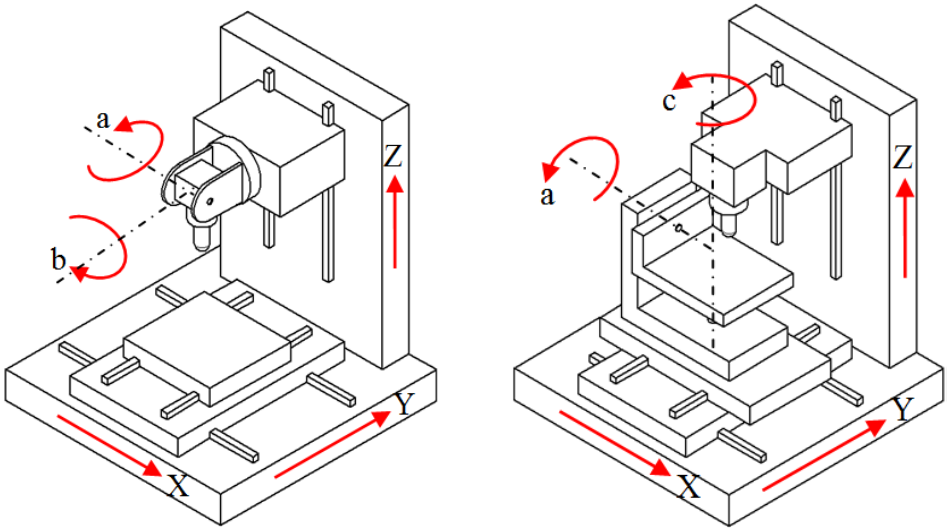

Figure 1: Standard configurations of the rotary axes on 5–axis CNC machines — an orientable–spindle machine (left) and orientable–table machine (right). For the former, the directions of the rotary axes that determine the spindle orientation are specified by (14). For the latter, the directions of the rotary axes that determine the workpiece table orientation are specified by (15).

The inverse kinematics problem, addressed by the rotary–axes real–time interpolator, amounts to determining the increments to the current rotary–axis orientations that are required during each sampling interval Δt of the servosystem, in order to maintain a desired relative orientation of the tool and workpiece. In some cases, it is possible to determine the rotary–axis inputs as continuous closed–form expressions in the path parameter ξ, that can be sampled through increments $\Delta\xi$ determined by the feedrate (i.e., speed of the

tool along the path) and sampling interval Δt. In other cases, a discrete time–step scheme may be used to determine the required axis angular increments. For typical 5–axis CNC machines, with sampling frequencies f of 1–10 kHz or higher (and sampling intervals $\Delta t = 1/f = 0.001$–0.0001 second or smaller), simple first–order methods furnish sufficient accuracy for practical use.

A rotation of a vector through angle θ about an axis specified by the unit vector $\mathbf{m} = (m_x, m_y, m_z)$ is defined by its product with an orthogonal matrix

$$\mathbf{M} = \begin{bmatrix} m_{11} & m_{12} & m_{13} \\ m_{21} & m_{22} & m_{23} \\ m_{31} & m_{32} & m_{33} \end{bmatrix} \tag{16}$$

whose elements are given [7] by

$$\begin{aligned} m_{11} &= m_x^2 + (1 - m_x^2)\cos\theta\,, \\ m_{12} &= m_x m_y (1 - \cos\theta) - m_z \sin\theta\,, \\ m_{13} &= m_z m_x (1 - \cos\theta) + m_y \sin\theta\,, \\ m_{21} &= m_x m_y (1 - \cos\theta) + m_z \sin\theta\,, \\ m_{22} &= m_y^2 + (1 - m_y^2)\cos\theta\,, \\ m_{23} &= m_y m_z (1 - \cos\theta) - m_x \sin\theta\,, \\ m_{31} &= m_z m_x (1 - \cos\theta) - m_y \sin\theta\,, \\ m_{32} &= m_y m_z (1 - \cos\theta) + m_x \sin\theta\,, \\ m_{33} &= m_z^2 + (1 - m_z^2)\cos\theta\,. \end{aligned} \tag{17}$$

In the special case of rotations about the x, y, z axes, the instances $\mathbf{M}_x, \mathbf{M}_y, \mathbf{M}_z$ of this matrix become

$$\begin{bmatrix} 1 & 0 & 0 \\ 0 & \cos\theta & -\sin\theta \\ 0 & \sin\theta & \cos\theta \end{bmatrix}, \quad \begin{bmatrix} \cos\theta & 0 & \sin\theta \\ 0 & 1 & 0 \\ -\sin\theta & 0 & \cos\theta \end{bmatrix}, \quad \begin{bmatrix} \cos\theta & -\sin\theta & 0 \\ \sin\theta & \cos\theta & 0 \\ 0 & 0 & 1 \end{bmatrix}.$$

5 Orientable–spindle machine

Let α and β denote current orientations of the a and b rotary axes, relative to the "home" position $\alpha = \beta = 0$, corresponding to a spindle aligned with the z–direction. Note that finite rotations about the a and b axes commute — i.e., their order is immaterial to the current spindle orientation. From (14)

and (16)–(17), a rotation by angle α (with $\beta = 0$) about a, followed with a rotation by angle β (with $\alpha \neq 0$) about b, corresponds to the matrix product

$$\begin{bmatrix} \cos\beta & 0 & \sin\beta \\ 0 & 1 & 0 \\ -\sin\beta & 0 & \cos\beta \end{bmatrix} \begin{bmatrix} 1 & 0 & 0 \\ 0 & \cos\alpha & -\sin\alpha \\ 0 & \sin\alpha & \cos\alpha \end{bmatrix} .$$

On the other hand, a rotation by angle β (with $\alpha = 0$) about b, followed with a rotation by angle α (with $\beta \neq 0$) about a, corresponds to the product

$$\begin{bmatrix} \cos^2\beta + \sin^2\beta\cos\alpha & \sin\beta\sin\alpha & \sin\beta\cos\beta(\cos\alpha - 1) \\ -\sin\beta\sin\alpha & \cos\alpha & -\cos\beta\sin\alpha \\ \sin\beta\cos\beta(\cos\alpha - 1) & \cos\beta\sin\alpha & \sin^2\beta + \cos^2\beta\cos\alpha \end{bmatrix} \begin{bmatrix} \cos\beta & 0 & \sin\beta \\ 0 & 1 & 0 \\ -\sin\beta & 0 & \cos\beta \end{bmatrix} .$$

Both products reduce to the same orthogonal matrix, namely

$$\mathbf{M} \;=\; \begin{bmatrix} \cos\beta & \sin\alpha\sin\beta & \cos\alpha\sin\beta \\ 0 & \cos\alpha & -\sin\alpha \\ -\sin\beta & \sin\alpha\cos\beta & \cos\alpha\cos\beta \end{bmatrix} . \tag{18}$$

This matrix may be regarded as mapping the tool axis vector in the home position, namely $\mathbf{a} = \mathbf{k}$, to a general orientation specified by

$$\mathbf{a} \;=\; (a_x, a_y, a_z) \;=\; (\cos\alpha\sin\beta, -\sin\alpha, \cos\alpha\cos\beta) . \tag{19}$$

This expression defines the relation between the tool orientation vector $\mathbf{a}$ and the axis rotation angles α, β.

The tool–orientation strategy proposed in [6] assumes a fixed workpiece orientation and a variable–orientation tool, and is thus directly applicable to orientable–spindle machines. The tool axis vector $\mathbf{a}$ specified by (8) and (12) can be written as

$$\mathbf{a} \;=\; \cos\psi\,\mathbf{n} + \sin\psi\,(\cos\phi\,\mathbf{t} + \sin\phi\,\mathbf{u}) , \tag{20}$$

where the dependence of the Darboux frame vectors $(\mathbf{n}, \mathbf{t}, \mathbf{u})$ on ξ is given by (2)–(4), and the angle ϕ is specified as a function of ξ by (9). Note that the Darboux frame $(\mathbf{n}, \mathbf{t}, \mathbf{u})$ — and hence the tool axis $\mathbf{a}$ — is specified in the machine (x, y, z) coordinates, since the workpiece orientation is invariant.

Noting that $-\frac{1}{2}\pi < \alpha, \beta < +\frac{1}{2}\pi$, the rotary–axis angles may be expressed from (19) in terms of the components $a_x(\xi), a_y(\xi), a_z(\xi)$ of $\mathbf{a}(\xi)$ as

$$\alpha(\xi) \;=\; -\sin^{-1} a_y(\xi) , \quad \beta(\xi) \;=\; \tan^{-1} \frac{a_x(\xi)}{a_z(\xi)} . \tag{21}$$

Although this is an essentially closed–form solution for the rotary–axis inputs, it should be noted that the integral (9) does not admit an analytic reduction, except in trivial cases. In fact, the controller employs only a discrete sampling of the inputs (21), and sufficiently accurate sampled values can be obtained using first–order expansions in the increment $\Delta\xi$ of the path parameter.

Let $\Delta\mathbf{a}$ denote the change in $\mathbf{a}$ incurred by an increment[2] $\Delta\xi$ in the curve parameter ξ corresponding to one servosystem sampling interval Δt. In the following analysis, all quadratic and higher–order terms in $\Delta\xi$ are dropped, on the assumption that they are small compared to the linear terms. From (5), the variations in the Darboux frame vectors corresponding to a parameter increment $\Delta\xi$ are

$$\begin{aligned} \Delta\mathbf{n} &= (\tau_{\mathrm{g}}\mathbf{u} - \kappa_{\mathrm{n}}\mathbf{t})\,\sigma\Delta\xi\,, \\ \Delta\mathbf{t} &= (\kappa_{\mathrm{n}}\mathbf{n} + \kappa_{\mathrm{g}}\mathbf{u})\,\sigma\Delta\xi\,, \\ \Delta\mathbf{u} &= -(\tau_{\mathrm{g}}\mathbf{n} + \kappa_{\mathrm{g}}\mathbf{t})\,\sigma\Delta\xi\,, \end{aligned}$$

while the change in the angle (9) is

$$\Delta\phi \;=\; -\,\kappa_{\mathrm{g}}\,\sigma\Delta\xi\,.$$

Now for small $\Delta\xi$, we have

$$\cos(\phi+\Delta\phi) \;\approx\; \cos\phi - \Delta\phi\sin\phi\,, \qquad \sin(\phi+\Delta\phi) \;\approx\; \sin\phi + \Delta\phi\cos\phi\,,$$

so the change $\Delta\mathbf{a} = \mathbf{a}(\xi+\Delta\xi) - \mathbf{a}(\xi)$ in (20) may be expressed as

$$\Delta\mathbf{a} \;=\; \cos\psi\,\Delta\mathbf{n} \;+\; \sin\psi\,[\,\cos\phi\,\Delta\mathbf{t} + \sin\phi\,\Delta\mathbf{u} + (\cos\phi\,\mathbf{u} - \sin\phi\,\mathbf{t})\,\Delta\phi\,]\,.$$

On substituting for $\Delta\mathbf{n}, \Delta\mathbf{t}, \Delta\mathbf{u}$ and $\Delta\phi$ this reduces to

$$\Delta\mathbf{a} \;=\; [\,\sin\psi(\kappa_{\mathrm{n}}\cos\phi - \tau_{\mathrm{g}}\sin\phi)\,\mathbf{n} - \cos\psi(\kappa_{\mathrm{n}}\mathbf{t} - \tau_{\mathrm{g}}\mathbf{u})\,]\,\sigma\Delta\xi\,, \tag{22}$$

and one can verify from (20) and (22) that

$$\mathbf{a}\cdot\Delta\mathbf{a} \;=\; 0 \tag{23}$$

— as expected since $\mathbf{a}$ is, by definition, a unit vector.

[2]This increment is computed from the toolpath geometry and feedrate by the real–time interpolator for the translational machine axes.

The change (22) in the tool axis orientation (20) must be realized through incremental rotations $\Delta\alpha$ and $\Delta\beta$ of the spindle about the a and b axes, with directions $\mathbf{m}_a$ and $\mathbf{m}_b$ specified by (14). For $\Delta\alpha = O(\Delta\xi)$ and $\Delta\beta = O(\Delta\xi)$, we invoke the small–angle approximations $(\cos\Delta\alpha, \sin\Delta\alpha) \approx (1, \Delta\alpha)$ and $(\cos\Delta\beta, \sin\Delta\beta) \approx (1, \Delta\beta)$ to define the incremental rotation matrices

$$\mathbf{M}_a \;=\; \begin{bmatrix} 1 & \sin\beta\,\Delta\alpha & 0 \\ -\sin\beta\,\Delta\alpha & 1 & -\cos\beta\,\Delta\alpha \\ 0 & \cos\beta\,\Delta\alpha & 1 \end{bmatrix}, \quad \mathbf{M}_b \;=\; \begin{bmatrix} 1 & 0 & \Delta\beta \\ 0 & 1 & 0 \\ -\Delta\beta & 0 & 1 \end{bmatrix}.$$

To first order in $\Delta\xi$, the product $\mathbf{M} = \mathbf{M}_a\,\mathbf{M}_b = \mathbf{M}_b\,\mathbf{M}_a$ is then given by

$$\mathbf{M} \;=\; \begin{bmatrix} 1 & \sin\beta\,\Delta\alpha & \Delta\beta \\ -\sin\beta\,\Delta\alpha & 1 & -\cos\beta\,\Delta\alpha \\ -\Delta\beta & \cos\beta\,\Delta\alpha & 1 \end{bmatrix}. \tag{24}$$

The desired increments $\Delta\alpha$, $\Delta\beta$ are thus determined from the condition

$$\mathbf{M}\,\mathbf{a} \;=\; \mathbf{a} + \Delta\mathbf{a} \qquad \text{or} \qquad (\mathbf{M} - \mathbf{I})\,\mathbf{a} \;=\; \Delta\mathbf{a}\,, \tag{25}$$

where $\mathbf{I}$ is the 3×3 identity matrix, and thus

$$\mathbf{M} - \mathbf{I} \;=\; \begin{bmatrix} 0 & \sin\beta\,\Delta\alpha & \Delta\beta \\ -\sin\beta\,\Delta\alpha & 0 & -\cos\beta\,\Delta\alpha \\ -\Delta\beta & \cos\beta\,\Delta\alpha & 0 \end{bmatrix}. \tag{26}$$

Writing $\mathbf{a} = (a_x, a_y, a_z)$ and $\Delta\mathbf{a} = (\Delta a_x, \Delta a_y, \Delta a_z)$ the condition (25) is then equivalent to the three scalar equations

$$\begin{aligned} \sin\beta\,\Delta\alpha\; a_y + \Delta\beta\; a_z \;&=\; \Delta a_x\,, \\ -\sin\beta\,\Delta\alpha\; a_x - \cos\beta\,\Delta\alpha\; a_z \;&=\; \Delta a_y\,, \\ -\Delta\beta\; a_x + \cos\beta\,\Delta\alpha\; a_y \;&=\; \Delta a_z\,, \end{aligned}$$

for $\Delta\alpha$ and $\Delta\beta$. The second equation yields

$$\Delta\alpha \;=\; -\,\frac{\Delta a_y}{\sin\beta\,a_x + \cos\beta\,a_z}\,, \tag{27}$$

and using $a_x\Delta a_x + a_y\Delta a_y + a_z\Delta a_z = 0$ from (23), the first and third equations then give

$$\Delta\beta \;=\; \frac{\cos\beta\,\Delta a_x - \sin\beta\,\Delta a_z}{\sin\beta\,a_x + \cos\beta\,a_z}\,. \tag{28}$$

Writing $\mathbf{n} = (n_x, n_y, n_z)$, $\mathbf{t} = (t_x, t_y, t_z)$, $\mathbf{u} = (u_x, u_y, u_z)$ the components of $\Delta\mathbf{a}$ and $\mathbf{a}$ in (27)–(28) are obtained from (20) and (22) as

$$\begin{aligned}
a_x &= \cos\psi\, n_x + \sin\psi\,(\cos\phi\, t_x + \sin\phi\, u_x)\,, \\
a_y &= \cos\psi\, n_y + \sin\psi\,(\cos\phi\, t_y + \sin\phi\, u_y)\,, \\
a_z &= \cos\psi\, n_z + \sin\psi\,(\cos\phi\, t_z + \sin\phi\, u_z)\,, \\
\Delta a_x &= [\,\sin\psi(\kappa_{\rm n}\cos\phi - \tau_{\rm g}\sin\phi)\, n_x - \cos\psi(\kappa_{\rm n} t_x - \tau_{\rm g} u_x)\,]\,\sigma\Delta\xi\,, \\
\Delta a_y &= [\,\sin\psi(\kappa_{\rm n}\cos\phi - \tau_{\rm g}\sin\phi)\, n_y - \cos\psi(\kappa_{\rm n} t_y - \tau_{\rm g} u_y)\,]\,\sigma\Delta\xi\,, \\
\Delta a_z &= [\,\sin\psi(\kappa_{\rm n}\cos\phi - \tau_{\rm g}\sin\phi)\, n_z - \cos\psi(\kappa_{\rm n} t_z - \tau_{\rm g} u_z)\,]\,\sigma\Delta\xi\,.
\end{aligned}$$

It is understood, in expressions (27)–(28), that σ, $\mathbf{n}$, $\mathbf{t}$, $\mathbf{u}$, $\kappa_{\rm n}$, $\tau_{\rm g}$, and ϕ are all evaluated at the current ξ. Note that these expressions become singular if $\sin\beta\, a_x + \cos\beta\, a_z = 0$. From (19) we observe that this corresponds to the circumstance $\cos\alpha = 0$, i.e., $\alpha = \pm\frac{1}{2}\pi$ and the tool is parallel to the y–axis. The angular range of the a axis will typically be constrained by software or hardware limits to preclude this circumstance.

Starting with a given initial tool axis orientation, defined by (20) with a particular choice for ϕ_0 in (9), the rotary axis inputs for a path step $\Delta\xi$ are determined from (27) and (28), and the process is repeated after incrementing ξ by $\Delta\xi$. In this manner, the coordinated translational and rotational tool motions that realize the scheme proposed in [6] are achieved.

Note that, if $\Delta\mathbf{a}$ is computed from (25) using the matrix defined by (26) and (27)–(28) and the current β value, $\mathbf{a} + \Delta\mathbf{a}$ is no longer precisely a unit vector. Since we are only concerned with the tool orientation, it can be unitized at each step $\Delta\xi$ through division by $|\mathbf{a}+\Delta\mathbf{a}|$. However, it is perhaps preferable to compute $\mathbf{a} + \Delta\mathbf{a}$ by using $\alpha + \Delta\alpha$, $\beta + \Delta\beta$ in (19), since it is then guaranteed to be always of unit magnitude.

Example 1. To assess the accuracy of the incremental inverse–kinematics scheme for the rotary axes of an orientable–spindle machine, we compare its output with the known variation of $\mathbf{a}$ for a non–trivial example that admits an exact closed–form solution [6]. Consider, on the torus defined for $R > r$ and $u, v \in [\,0, 2\pi\,]$ by

$$\mathbf{s}(u, v) \;=\; ((R + r\cos v)\cos u, (R + r\cos v)\sin u, r\sin v)\,, \tag{29}$$

the path $\mathbf{r}(\xi) = \mathbf{s}(u(\xi), v(\xi))$ from $\mathbf{r}(0) = \mathbf{s}(0, 0) = (R + r, 0, 0)$ to $\mathbf{r}(1) = \mathbf{s}(\frac{1}{2}\pi, \frac{1}{2}\pi) = (0, R, r)$ specified by

$$(u(\xi), v(\xi)) \;=\; (\tfrac{1}{2}\pi\xi, \tfrac{1}{2}\pi\xi) \tag{30}$$

for $\xi \in [\,0,1\,]$. Figure 2 shows this path on the torus (29) with $R = 2$, $r = 1$ and the surface normals

$$\mathbf{n} \;=\; \frac{\mathbf{s}_u \times \mathbf{s}_v}{|\,\mathbf{s}_u \times \mathbf{s}_v\,|} \;=\; (\cos u \cos v, \sin u \cos v, \sin v) \tag{31}$$

along it. For the path (30), we have

$$\mathbf{r}'(\xi) \;=\; u'(\xi)\,\mathbf{s}_u(u(\xi), v(\xi)) \;+\; v'(\xi)\,\mathbf{s}_v(u(\xi), v(\xi))$$

and the parametric speed is

$$\sigma(\xi) \;=\; |\mathbf{r}'(\xi)| \;=\; \tfrac{1}{2}\pi\,\eta(\xi)\,, \quad \eta(\xi) \;=\; \sqrt{(R + r\cos v(\xi))^2 + r^2}\,.$$

We henceforth omit the dependence u, v, σ, η on ξ. The tangent $\mathbf{t} = (t_x, t_y, t_z) = \mathbf{r}'/\sigma$ and tangent normal $\mathbf{u} = (u_x, u_y, u_z) = \mathbf{n} \times \mathbf{t}$ along (30) are defined by

$$\begin{aligned}
\eta\, t_x &= -\,(R + r\cos v)\sin u - r\cos u \sin v\,, \\
\eta\, t_y &= (R + r\cos v)\cos u - r \sin u \sin v\,, \\
\eta\, t_z &= r\cos v\,, \qquad\qquad (32) \\
\eta\, u_x &= r\sin u - (R + r\cos v)\cos u \sin v\,, \\
\eta\, u_y &= -\,r\cos u - (R + r\cos v)\sin u \sin v\,, \\
\eta\, u_z &= (R + r\cos v)\cos v\,, \qquad\qquad (33)
\end{aligned}$$

and from (6) the normal curvature, geodesic curvature, and geodesic torsion can be expressed as

$$\kappa_{\rm n} \;=\; -\,\frac{R\cos v + r(1 + \cos^2 v)}{(R + r\cos v)^2 + r^2}\,,$$

$$\kappa_{\rm g} \;=\; \frac{\sin v}{\sqrt{(R + r\cos v)^2 + r^2}}\,\left[\,1 + \frac{r^2}{(R + r\cos v)^2 + r^2}\,\right]\,,$$

$$\tau_{\rm g} \;=\; \frac{R}{(R + r\cos v)^2 + r^2}\,.$$

It was shown in [6] that, for this example, the angle function (9) is given by

$$\phi(\xi) \;=\; \phi_0 + \cos\tfrac{1}{2}\pi\xi - 1 + \tan^{-1}\left(\frac{R}{r} + \cos\tfrac{1}{2}\pi\xi\right) - \tan^{-1}\left(\frac{R}{r} + 1\right)\,. \tag{34}$$

For the inclination angle $\psi = \frac{1}{4}\pi$, the variation of the tool axis defined by (20) and (34) along the path (30) is illustrated in Figure 2.

To compute the axis angles $\alpha(\xi)$, $\beta(\xi)$ and corresponding tool orientation $\mathbf{a}(\xi)$ along the path (30) on the torus (29) incrementally using (27)–(28), the initial orientation $\mathbf{a}(0) = (a_x(0), a_y(0), a_z(0))$ is first determined from (9) and (20) with $\phi_0 = 0$. The initial axis angles $\alpha(0)$, $\beta(0)$ are then determined by invoking (19) to obtain

$$\alpha(0) \;=\; \sin^{-1} a_y(0)\,, \quad \beta(0) \;=\; \tan^{-1} \frac{a_x(0)}{a_z(0)}\,.$$

In the present case $\alpha(0) = -42.1°$, $\beta(0) = 72.5°$. With this initial condition, Figure 3 shows the variation of the axis angles α and β along the path on the torus, computed using (27)–(28) with the increment $\Delta\xi = 0.001$.

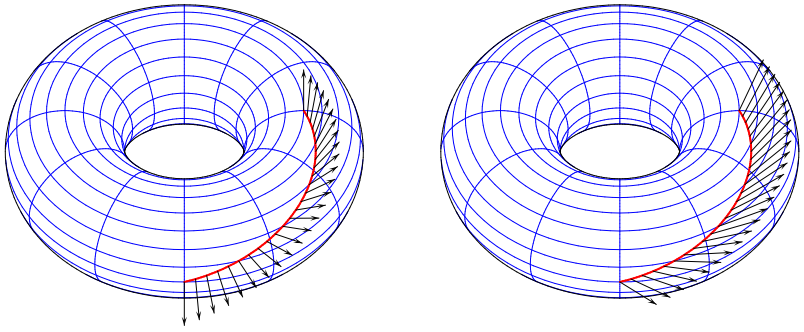

Figure 2: The path specified by (30) on the torus (29), with $R = 2$ and $r = 1$, showing the surface normal $\mathbf{n}$ (left) the tool axis $\mathbf{a}$ (right) along this path.

If $\mathbf{a}$ is the exact tool axis vector and $\tilde{\mathbf{a}}$ is the (unitized) tool axis vector, computed for any given parameter increment $\Delta\xi$ by the inverse–kinematics scheme described above, we define for each ξ the non–negative error measure

$$\epsilon \;=\; 1 - \tilde{\mathbf{a}} \cdot \mathbf{a}\,, \tag{35}$$

satisfying $\epsilon = 0$ if and only if $\tilde{\mathbf{a}} = \mathbf{a}$. Figure 4 illustrates the variation of the error measure (35) for parameter increments $\Delta\xi = 0.001$ and $\Delta\xi = 0.0001$. Note that the value $\epsilon = 10^{-6}$ corresponds to an angular deviation of $\sim 0.08°$, while $\epsilon = 10^{-8}$ corresponds to $\sim 0.008°$.

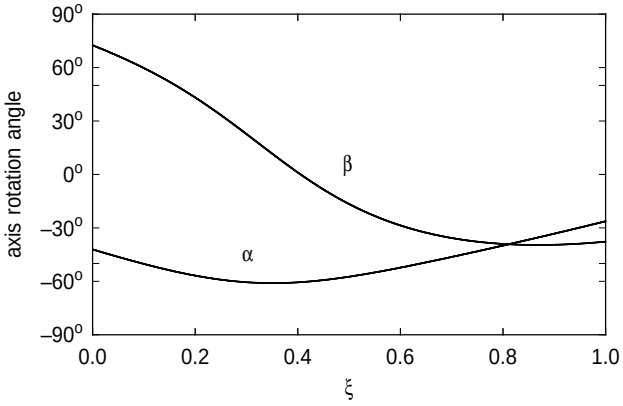

Figure 3: Variation of the rotary–axis angles α, β along the path (30) on the torus (29), computed incrementally from (27)–(28), for an orientable–spindle machine with initial spindle orientation defined by (9) and (20) with $\phi_0 = 0$.

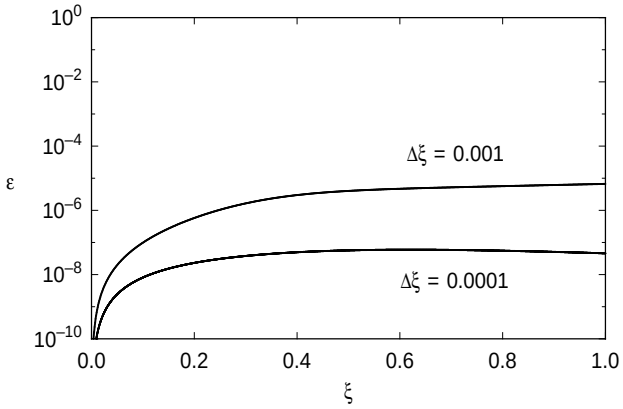

Figure 4: The error measure (35) for discrete computation of the tool axis along the path (30) on the torus (29) for step sizes $\Delta\xi = 0.001$ and 0.0001.

6 Orientable–table machine

The optimal tool orientation scheme developed in [6] implicitly assumes a fixed workpiece orientation, and is directly applicable to orientable–spindle machines. In the context of orientable–table machines, however, it requires a re–interpretation. The method may be regarded as constraining the *relative* orientation of the tool axis and surface normal at the tool contact point. In [6], the surface normal $\mathbf{n}$ is employed as a reference, and the tool axis $\mathbf{a}$ is decomposed into components $\mathbf{a}_\parallel$ and $\mathbf{a}_\perp$ parallel and perpendicular to it. The parallel component is just $\mathbf{a}_\parallel = \cos\psi\,\mathbf{n}$, while the perpendicular component $\mathbf{a}_\perp$ is required to exhibit no instantaneous rotation about $\mathbf{n}$.

In the context of an orientable–table machine, the tool axis $\mathbf{a}$ is fixed and the workpiece (and with it the surface normal $\mathbf{n}$) rotates about the c and a axes. In this context, it is preferable to choose the tool axis $\mathbf{a}$ as a reference, and decompose the surface normal into components $\mathbf{n}_\parallel$ and $\mathbf{n}_\perp$ parallel and perpendicular to it. The desired relative motion of $\mathbf{a}$ and $\mathbf{n}$ is then achieved if $\mathbf{n}_\parallel = \mathbf{a}\cos\psi$ and $\mathbf{n}_\perp$ exhibits no instantaneous rotation about $\mathbf{a}$. Since $\mathbf{a}$ is aligned with the machine z–axis, this means that the actuation of the rotary axes must be such as to align the surface normal $\mathbf{n}$ at the tool contact point with a *fixed unit vector* $\mathbf{n}_0$ in the machine (x, y, z) coordinate system, as the contact point traverses the given toolpath. Any departure from this condition incurs a change of workpiece orientation that is superfluous to maintenance of a fixed angle ψ between the tool axis $\mathbf{a}$ and surface normal $\mathbf{n}$.

The fixed vector $\mathbf{n}_0$ can be expressed, for some chosen angle ζ, as

$$\mathbf{n}_0 \;=\; \sin\psi\,(\cos\zeta\,\mathbf{i} + \sin\zeta\,\mathbf{j}) + \cos\psi\,\mathbf{k}\,.$$

For brevity, we henceforth assume $\zeta = 0$ without loss of generality, so $\mathbf{n}_0 = \sin\psi\,\mathbf{i} + \cos\psi\,\mathbf{k}$. The surface must be initially oriented so that the normal $\mathbf{n}(0)$ at the toolpath start point $\mathbf{r}(0) = \mathbf{s}(u(0), v(0))$ is aligned with $\mathbf{n}_0$.

Let γ and α denote current orientations of the c and a rotary axes, relative to the "home" position $\gamma = \alpha = 0$, corresponding to a horizontal table whose sides are aligned with the x, y directions. From (15) and (16)–(17), a rotation by angle α (with $\gamma = 0$) about a, followed with a rotation by angle γ (with $\alpha \neq 0$) about c, corresponds to the matrix product

$$\begin{bmatrix} \cos\gamma & -\sin\gamma & 0 \\ \sin\gamma & \cos\gamma & 0 \\ 0 & 0 & 1 \end{bmatrix} \begin{bmatrix} 1 & 0 & 0 \\ 0 & \cos\alpha & -\sin\alpha \\ 0 & \sin\alpha & \cos\alpha \end{bmatrix} .$$

On the other hand, a rotation by angle γ (with $\alpha = 0$) about c, followed with a rotation by angle α (with $\gamma \neq 0$) about a, corresponds to the product

$$\begin{bmatrix} \cos^2\gamma + \sin^2\gamma\cos\alpha & \sin\gamma\cos\gamma(1-\cos\alpha) & \sin\gamma\sin\alpha \\ \sin\gamma\cos\gamma(1-\cos\alpha) & \sin^2\gamma + \cos^2\gamma\cos\alpha & -\cos\gamma\sin\alpha \\ -\sin\gamma\sin\alpha & \cos\gamma\sin\alpha & \cos\alpha \end{bmatrix} \begin{bmatrix} \cos\gamma & -\sin\gamma & 0 \\ \sin\gamma & \cos\gamma & 0 \\ 0 & 0 & 1 \end{bmatrix} .$$

Both products reduce to the same orthogonal matrix, namely

$$\mathbf{M} \;=\; \begin{bmatrix} \cos\gamma & -\sin\gamma\cos\alpha & \sin\gamma\sin\alpha \\ \sin\gamma & \cos\gamma\cos\alpha & -\cos\gamma\sin\alpha \\ 0 & \sin\alpha & \cos\alpha \end{bmatrix} . \tag{36}$$

Hence, finite rotations about the c and a axes commute — i.e., their order is immaterial to the current workpiece table orientation.

It is convenient to write $\mathbf{n}$ in terms of spherical polar coordinate angles (ϑ, φ) with $0 \leq \vartheta \leq \pi$ and $0 \leq \varphi \leq 2\pi$ as

$$(n_x, n_y, n_z) \;=\; (\cos\vartheta, \sin\vartheta\cos\varphi, \sin\vartheta\sin\varphi) , \tag{37}$$

where $\cos\vartheta = n_x$, $\sin\vartheta = \sqrt{n_y^2 + n_z^2}$ and $(\cos\varphi, \sin\varphi) = (n_y, n_z)/\sqrt{n_y^2 + n_z^2}$. The goal is to continuously orient the workpiece, by appropriate variations of the rotary–axis angles γ and α, so that the surface normal $\mathbf{n}$ at the contact point is always aligned with the fixed vector $\mathbf{n}_0 = \sin\psi\,\mathbf{i} + \cos\psi\,\mathbf{k}$.

Let $\gamma(\xi)$ and $\alpha(\xi)$ be the angular positions of the c and a axes required to align the surface normal $\mathbf{n}(\xi) = (n_x(\xi), n_y(\xi), n_z(\xi))$ at the point $\mathbf{r}(\xi)$ of the toolpath with the fixed vector $\mathbf{n}_0 = \sin\psi\,\mathbf{i} + \cos\psi\,\mathbf{k}$ — i.e., $\mathbf{M}(\xi)\,\mathbf{n}(\xi) = \mathbf{n}_0$, where $\mathbf{M}(\xi)$ is the matrix defined by substituting $\gamma(\xi)$ and $\alpha(\xi)$ in (36). This matrix can be regarded as the solution of a system of first–order differential equations (see the Appendix). Alternatively, one can solve for $\gamma(\xi)$ and $\alpha(\xi)$ algebraically by noting that they must satisfy

$$\begin{aligned} \cos\gamma(\xi)\,n_x(\xi) - \sin\gamma(\xi)\,(\cos\alpha(\xi)\,n_y(\xi) - \sin\alpha(\xi)\,n_z(\xi)) \;&=\; \sin\psi\,, \\ \sin\gamma(\xi)\,n_x(\xi) + \cos\gamma(\xi)\,(\cos\alpha(\xi)\,n_y(\xi) - \sin\alpha(\xi)\,n_z(\xi)) \;&=\; 0\,, \\ \sin\alpha(\xi)\,n_y(\xi) + \cos\alpha(\xi)\,n_z(\xi) \;&=\; \cos\psi\,. \end{aligned}$$

Substituting from (37), these equations can be re–formulated as

$$\begin{aligned} \cos\gamma(\xi)\,\cos\vartheta(\xi) - \sin\gamma(\xi)\,\sin\vartheta(\xi)\,\cos(\alpha(\xi)+\varphi(\xi)) \;&=\; \sin\psi\,, \\ \sin\gamma(\xi)\,\cos\vartheta(\xi) + \cos\gamma(\xi)\,\sin\vartheta(\xi)\,\cos(\alpha(\xi)+\varphi(\xi)) \;&=\; 0\,, \\ \sin\vartheta(\xi)\,\sin(\alpha(\xi)+\varphi(\xi)) \;&=\; \cos\psi\,. \end{aligned} \tag{38}$$

Adding the first and second equations, multiplied with $\cos\gamma(\xi)$ and $\sin\gamma(\xi)$ respectively, then gives

$$\cos\gamma(\xi) \;=\; \frac{\cos\vartheta(\xi)}{\sin\psi}\,. \tag{39}$$

Using this in conjunction with the second and third equations, we obtain

$$\cos(\alpha(\xi)+\varphi(\xi)) \;=\; -\,\frac{\sin\psi\,\sin\gamma(\xi)}{\sin\vartheta(\xi)}\,, \quad \sin(\alpha(\xi)+\varphi(\xi)) \;=\; \frac{\cos\psi}{\sin\vartheta(\xi)}\,. \tag{40}$$

However, the orientable–table machine can achieve the desired motion only under certain restrictions on the variation of the surface normal $\mathbf{n}$ along the given toolpath. Since $0 \le \vartheta(\xi) \le \pi$ and $0 < \psi < \frac{1}{2}\pi$, equation (39) and the second of equations (40) can only be satisfied when

$$|\cos\vartheta(\xi)| \;\le\; \sin\psi \qquad \text{and} \qquad \sin\vartheta(\xi) \;\ge\; \cos\psi\,,$$

and the first of equations (40) can then also be satisfied. These two conditions are equivalent to the constraint

$$\tfrac{1}{2}\pi - \psi \;\le\; \vartheta(\xi) \;\le\; \tfrac{1}{2}\pi + \psi \tag{41}$$

on the range of $\vartheta(\xi)$, i.e., the surface normal $\mathbf{n}(\xi)$ must lie outside a cone of half–angle $\frac{1}{2}\pi - \psi$ about the positive/negative x–direction. The constraint (41) must be satisfied at each point of the toolpath, to ensure that $\gamma(\xi)$ and $\alpha(\xi)$ are properly defined by equations (39)–(40), and the machine is thus capable of maintaining the desired relative tool/workpiece orientation.

In general, equation (39) determines two possible values $\gamma_1(\xi), \gamma_2(\xi)$ in the interval $(-\pi, +\pi\,]$ that differ only in sign. Since $\gamma_2(\xi) = -\,\gamma_1(\xi)$, equations (40) give corresponding values $\alpha_1(\xi)$, $\alpha_2(\xi) = \pi - \alpha_1(\xi) - 2\,\varphi(\xi)$. Depending on $\varphi(\xi)$, however, they may not both lie in the allowed interval $[\,-\frac{1}{2}\pi, +\frac{1}{2}\pi\,]$ for $\alpha(\xi)$. For example, when $\varphi(\xi) = 0$ and $\alpha_1(\xi) \in [\,-\frac{1}{2}\pi, +\frac{1}{2}\pi\,]$, then $\alpha_2(\xi) \in [\,\frac{1}{2}\pi, +\frac{3}{2}\pi\,]$ so $\gamma_1(\xi), \alpha_1(\xi)$ is the only feasible solution. On the other hand, if $\varphi(\xi) = \frac{1}{2}\pi$ and $\alpha_1(\xi) \in [\,-\frac{1}{2}\pi, +\frac{1}{2}\pi\,]$, then $\alpha_2(\xi) \in [\,-\frac{1}{2}\pi, +\frac{1}{2}\pi\,]$ so $\gamma_1(\xi), \alpha_1(\xi)$ and $\gamma_2(\xi), \alpha_2(\xi)$ are both feasible solutions that map $\mathbf{n}(\xi)$ onto $\mathbf{n}_0$.

The motion should employ inputs $\gamma(\xi)$ and $\alpha(\xi)$ that specify *continuous* variations of the rotary–axis angles with the path parameter ξ, so as to align the surface normal $\mathbf{n}(\xi)$ with the fixed vector $\mathbf{n}_0$. To initialize the motion, the rotary axes must be set to the positions $\gamma(0)$ and $\alpha(0)$ defined with $\xi = 0$ in (39)–(40), to align the initial surface normal $\mathbf{n}(0)$ with $\mathbf{n}_0$.

In the case of an orientable–table machine, the rotary–axis inputs γ and α that realize the optimal relative tool/workpiece orientation scheme proposed in [6] admit an essentially closed–form solution. Note that the function $\phi(\xi)$ defined by (9) is not required in the orientable–table context. In the case of an orientable–spindle machine, $\phi(\xi)$ compensates for the non–zero angular velocity component of the Darboux frame — which is employed to specify the tool orientation — in the surface normal direction. The inverse kinematics of the orientable–table machine is a simpler problem, since it is only concerned with the orientation of the surface normal, relative to a fixed reference frame, along the toolpath. However, the existence of solutions is contingent upon constraints on the variation of the surface normal along the toolpath.

Example 2. Consider the torus of Example 1 for the case of the orientable–table machine. Since condition (41) is not satisfied along the path (30) when $\xi \in [\,0,1\,]$ we use $\xi \in [\,\frac{1}{2},\frac{3}{2}\,]$ instead. Comparing (31) and (37) yields

$$\cos\vartheta(\xi) \;=\; \cos^2\tfrac{1}{2}\pi\xi\,, \quad \sin\vartheta(\xi) \;=\; \sin\tfrac{1}{2}\pi\xi\sqrt{1+\cos^2\tfrac{1}{2}\pi\xi}\,,$$

$$\cos\varphi(\xi) \;=\; \frac{\cos\frac{1}{2}\pi\xi}{\sqrt{1+\cos^2\frac{1}{2}\pi\xi}}\,, \quad \sin\varphi(\xi) \;=\; \frac{1}{\sqrt{1+\cos^2\frac{1}{2}\pi\xi}}\,.$$

Then the rotary–axis inputs $\gamma(\xi)$ and $\alpha(\xi)$ are defined by substituting these expressions into (39) and (40). In particular, we use the angle $\gamma(\xi)$ satisfying (39) within the interval $[\,0,\pi\,]$. Figure 5 illustrates the variations of the axis angles γ and α with the path parameter ξ computed in this manner.

The computation of the rotary–axis inputs is much simpler in this case than for the orientable–spindle machine case described in Example 1, since it is not necessary to invoke the Darboux frame apparatus (5) and the function (9). Note, however, that the path (30) with $\xi \in [\,0,1\,]$ employed in Example 1 is infeasible on the orientable–table machine, since the initial surface normal $\mathbf{n}(0) = (1,0,0)$ violates the condition (41). In the present context, a modified parameter interval $\xi \in [\,\frac{1}{2},\frac{3}{2}\,]$ was necessary to ensure a feasible solution.

Figure 6 shows how the position/orientation of the torus is varied, using the toolpath $\mathbf{r}(\xi)$ and rotary–axis inputs $\gamma(\xi)$ and $\alpha(\xi)$ computed above, so as to ensure that the surface normal $\mathbf{n}(\xi)$ at the contact point is transformed into a fixed vector in the machine coordinate system.

Figure 7 illustrates the inverse kinematics of an orientable–table machine for a smooth path on a tensor–product bicubic NURBS surface, implemented

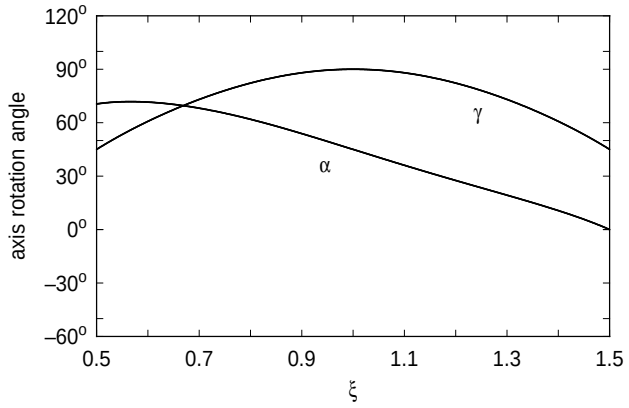

Figure 5: Variation of the rotary–axis angles γ, α along the path (30) on the torus (29), computed from (39) and (40), for the orientable–table machine.

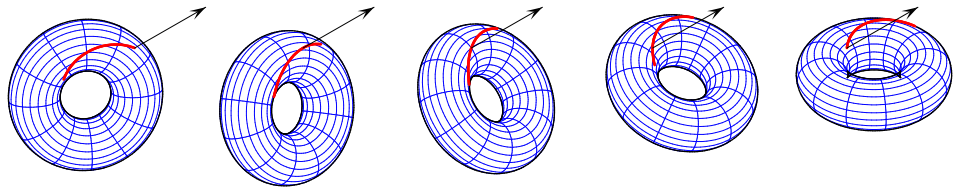

Figure 6: The toolpath (30) for $\xi \in [\,\frac{1}{2}, \frac{3}{2}\,]$ on the torus (29) for the case of an orientable–table machine in Example 2. The position and orientation of the torus vary continuously, such that the surface normal (shown as an arrow) at the tool contact point is a fixed vector in the machine coordinate system.

using the OpenNURBS and OpenSceneGraph software libraries. The surface parameter domain was normalized to $(u, v) \in [\,0, 1\,] \times [\,0, 1\,]$ and the tool path $\mathbf{r}(\xi) = \mathbf{s}(u(\xi), v(\xi))$ was defined as a line segment in the parameter domain, between the points $\mathbf{r}(0) = \mathbf{s}(0, 0)$ and $\mathbf{r}(1) = \mathbf{s}(0.8, 0.8)$.

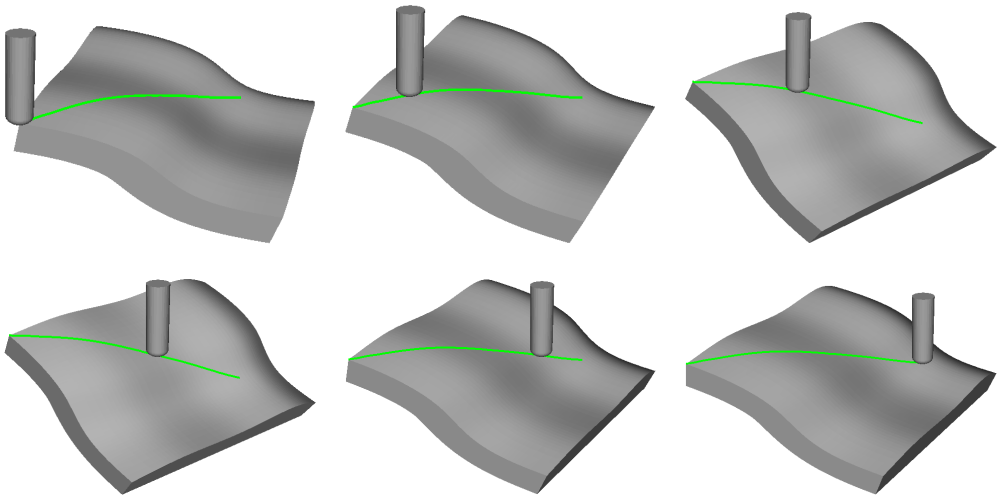

Figure 7: Variation of the workpiece orientation for a smooth toolpath $\mathbf{r}(\xi)$ on a bicubic NURBS surface. The workpiece orientations at the path parameter values $\xi = 0.0, 0.2, 0.4, 0.6, 0.8, 1.0$ are shown, from top left to bottom right.

The limitation on the toolpaths incurred by the orientable–table machine, to ensure satisfaction of the condition (41), can be alleviated by re–fixturing the workpiece on the machine table with a different orientation. However, use of multiple re–fixturings during machining operations is undesirable, because of inaccuracies they incur in registering the workpiece location/orientation.

7 Closure

The problem of determining the rotary–axis inputs to 5–axis CNC machines, so as to minimize variations of relative tool/workpiece orientation under the constraint of a fixed cutting speed with a ball–end tool, has been addressed. The results of a prior study [6] can be directly applied to orientable–spindle machines to determine the axis inputs, but since they depend on the integral of the geodesic curvature along the toolpath, a discrete time–step procedure

was proposed that offers sufficiently accurate real–time computation at the typical sampling frequencies of modern 5–axis CNC machines.

The results of [6] require re–interpretation in the context of an orientable–table machine. In this case, the tool axis is stationary, and the minimization of variations in the relative tool/workpiece orientation implies that the table on which the workpiece is mounted must be continuously re–oriented so that the surface normal at the tool contact point becomes a static vector in the machine coordinate system. A closed–form solution for the rotary–axis inputs realizing this motion is possible, that does not incur any irreducible integrals. However, the desired motion can only be realized when certain constraints on the variation of the surface normal along the toolpath are satisfied.

The elimination of "unnecessary" rotary–axis actuation in 5–axis CNC machining of free–form surfaces, subject to toolpath geometry and cutting–speed constraints, can enhance the efficiency and accuracy of an expensive and time–consuming fabrication process. The measure of optimality adopted herein is essentially differential in nature — comparing the tool axis $\mathbf{a}$ and surface normal $\mathbf{n}$ at the contact point, we require the component of one vector parallel to the other to maintain the fixed value $\cos\psi$, while the perpendicular component must exhibit no instantaneous rotation about the other.

The formulation of alternative measures of optimality, expressed in terms of a suitable combined metric for the rotary–axis inputs on a given machine configuration, is worthy of further detailed investigation.

Appendix

For a given unit vector $\mathbf{n}(\xi)$, let $\mathbf{M}(\xi)$ be a rotation matrix of the form (36) that maps $\mathbf{n}(\xi)$ into a fixed vector, i.e., $\tilde{\mathbf{n}} = \mathbf{M}\,\mathbf{n}$ satisfies $\tilde{\mathbf{n}}' = \mathbf{M}'\,\mathbf{n} + \mathbf{M}\,\mathbf{n}' = \mathbf{0}$. Since $\mathbf{M}$ is an orthogonal matrix, this condition can be expressed as

$$\mathbf{M}^T\mathbf{M}'\,\mathbf{n} \,+\, \mathbf{n}' \,=\, \mathbf{0}\,. \tag{42}$$

For the rotation matrix (36), one can verify that

$$\mathbf{M}^T\mathbf{M}' \,=\, \begin{bmatrix} 0 & -\gamma'\cos\alpha & \gamma'\sin\alpha \\ \gamma'\cos\alpha & 0 & -\alpha' \\ -\gamma'\sin\alpha & \alpha' & 0 \end{bmatrix},$$

and equation (42) can be re–written as

$$\boldsymbol{\omega} \times \mathbf{n} \,=\, \mathbf{n}'\,,$$

where $\boldsymbol{\omega} = -(\alpha', \sin\alpha\,\gamma', \cos\alpha\,\gamma')$. This is equivalent to the scalar equations

$$\begin{aligned}(n_y\cos\alpha - n_z\sin\alpha)\,\gamma' &= n_x'\,,\\ n_z\alpha' - n_x\cos\alpha\,\gamma' &= n_y'\,,\\ n_x\sin\alpha\,\gamma' - n_y\alpha' &= n_z'\,.\end{aligned}$$

However, these equations are not independent: multiplying them by n_x, n_y, n_z and adding gives $n_x n_x' + n_y n_y' + n_z n_z' = \mathbf{n}\cdot\mathbf{n}' = 0$, a consequence of the fact that $\mathbf{n}$ is unit vector. Using this fact, the equations reduce to

$$\alpha' \;=\; \frac{n_y'\sin\alpha + n_z'\cos\alpha}{n_z\sin\alpha - n_y\cos\alpha}\,, \qquad \gamma' \;=\; \frac{n_x'}{n_y\cos\alpha - n_z\sin\alpha}\,. \tag{43}$$

The first equation in (43) gives $(\sin\alpha\, n_y + \cos\alpha\, n_z)' = 0$, and using (37) this can be expressed as $(\sin\vartheta\sin(\alpha+\varphi))' = 0$. Hence, we have

$$\sin(\alpha+\varphi) \;=\; \frac{\cos\psi}{\sin\vartheta} \tag{44}$$

for some constant $\cos\psi$, provided that the condition (41) holds. Again using (37), the second equation reduces to

$$\cos(\alpha+\varphi)\,\gamma' \;+\; \vartheta' \;=\; 0\,. \tag{45}$$

Substituting from (44) and (45) into $\sin^2(\alpha+\varphi)+\cos^2(\alpha+\varphi) = 1$ then gives

$$\gamma' \;=\; \pm\frac{\sin\vartheta\;\vartheta'}{\sqrt{\sin^2\vartheta - \cos^2\psi}} \;=\; \mp\frac{(\cos\vartheta)'}{\sqrt{\sin^2\psi - \cos^2\vartheta}}\,.$$

Setting $u = \cos\vartheta$, the above relation can be integrated to obtain

$$\gamma \;=\; \gamma_0 \;\mp\; \sin^{-1}\frac{\cos\vartheta}{\sin\psi}\,,$$

and with the choice $\gamma_0 = \frac{1}{2}\pi$ for the integration constant, this gives

$$\cos\gamma \;=\; \pm\frac{\cos\vartheta}{\sin\psi} \tag{46}$$

Finally, substituting (44) and (46) in $\cos^2(\alpha+\varphi) = 1-\sin^2(\alpha+\varphi)$, we obtain

$$\cos(\alpha+\varphi) \;=\; \mp\frac{\sin\psi\;\sin\gamma}{\sin\vartheta}\,. \tag{47}$$

Note that the combinations of signs indicated in (46) and (47) are necessary to ensure satisfaction of (43). The solutions given previously in expressions (39) and (40) correspond to the first sign choice in (46) and (47).

References

[1] R. L. Bishop (1975), There is more than one way to frame a curve, *Amer. Math. Monthly* **82**, 246–251.

[2] C. Castagnetti, E. Duc, and P. Ray (2008), The domain of admissible orientation concept: a new method for five–axis tool path optimisation, *Comput. Aided Design* **40**, 938–950.

[3] H. I. Choi and C. Y. Han (2002), Euler–Rodrigues frames on spatial Pythagorean–hodograph curves, *Comput. Aided Geom. Design* **19**, 603–620.

[4] R. T. Farouki (2010), Quaternion and Hopf map characterizations for the existence of rational rotation–minimizing frames on quintic space curves, *Adv. Comp. Math.* **33**, 331–348.

[5] R. T. Farouki, C. Giannelli, C. Manni, and A. Sestini (2012), Design of rational rotation–minimizing rigid body motions by Hermite interpolation, *Math. Comp.* **81**, 879–903.

[6] R. T. Farouki and S. Li (2013), Optimal tool orientation control for 5–axis CNC milling with ball-end cutters, *Comput. Aided Geom. Design* **30**, 226–239.

[7] I. D. Faux and M. J. Pratt (1979), *Computational Goemetry for Design and Mnaufacture*, Ellis Horwood Ltd, Chichester.

[8] P. Gray, S. Bedi, and F. Ismail (2003), Rolling ball method for 5–axis surface machining, *Comput. Aided Design* **35**, 347–357.

[9] H. Guggenheimer (1989), Computing frames along a trajectory, *Comput. Aided Geom. Design* **6**, 77–78.

[10] M. C. Ho, Y. R. Hwang, and C. H. Hu (2003), Five–axis tool orientation smoothing using quaternion interpolation algorithm, *Inter. J. Mach. Tools Manuf.* **43**, 1259–1267.

[11] Y. R. Hwang and C. S. Liang (1998), Cutting error analysis for spindle–tilting type five–axis NC machines, *Int. J. Adv. Manuf. Technol.* **14**, 399–405.

[12] C. S. Jun, K. Cha, and Y. S. Lee (2003), Optimizing tool orientations for 5–axis machining by configuration–space search method, *Comput. Aided Design* **35**, 549–566.

[13] Y. H. Jung, D. W. Lee, J. S. Kim, and H. S. Mok (2002), NC post–processor for 5–axis milling machine of table–rotating/tilting type, *J. Mater. Proc. Tech.* **130-131**, 641–646.

[14] F. Klok (1986), Two moving coordinate frames for sweeping along a 3D trajectory, *Comput. Aided Geom. Design* **3**, 217–229.

[15] E. Kreyszig (1959), *Differential Geometry*, University of Toronto Press.

[16] R–S. Lee and C–H. She (1997), Developing a postprocessor for three types of five–axis machine tools, *Int. J. Adv. Manuf. Technol.* **13**, 658–665.

[17] Y. S. Lee (1997), Admissible tool orientation control of gouging avoidance for 5–axis complex surface machining, *Comput. Aided Design* **29**, 507–521.

[18] N. Rao, F. Ismail, and S. Bedi (1997), Tool path planning for five–axis machining using the principal axis method, *Inter. J. Mach. Tools Manuf.* **37**, 1025–1040.

[19] S. Sakamoto and I. Inasaki (1993), Analysis of generating motion for five–axis machining centers, *Trans. Jpn. Soc. Mech. Engr.* Ser. C **59** (561), 1553–1559.

[20] D. J. Struik (1988), *Lectures on Classical Differential Geometry*, Dover Publications (reprint), New York.

[21] W. Wang, B. Jüttler, D. Zheng, and Y. Liu (2008), Computation of rotation minimizing frames, *ACM Trans. Graphics* **27**, No. 1, Article 2, 1–18.

[22] A. Warkentin, F. Ismail, and S. Bedi (2000), Comparison between multi–point and other 5–axis tool positioning strategies, *Inter. J. Mach. Tools Manuf.* **40**, 185–208.

[23] X. J. Xu, C. Bradley, Y. F. Zhang, H. T. Loh, and Y. S. Wong (2002), Tool–path generation for five–axis machining of free–form surfaces based on accessibility analysis, *Inter. J. Prod. Res.* **40**, 3253–3274.